Available online at www.sciencedirect.com
SCIENCE DIRECT®
Journal of Chromatography A, 1055 (2004) 1–9
JOURNAL OF CHROMATOGRAPHY A
www.elsevier.com/locate/chroma

Construction and application of a stoichiometric displacement model for retention in chiral recognition of molecular imprinting

Ruifeng Sun, Huimin Yu**, Hui Luo, Zhongyao Shen*

Department of Chemical Engineering, Institute of Biomechanical Engineering, Tsinghua University, Beijing 100084, PR China

Received 1 June 2004; received in revised form 5 August 2004; accepted 9 August 2004

Abstract

To do an extensive investigation of the chiral recognition mechanism of the molecular imprinting technique, two kinds of enantio-selective molecularly imprinted polymers (MIPs), *N*-*tert*-butoxycarbonyl-L-tryptophan (*N*-Boc-L-Trp) and *N*-*tert*-butoxycarbonyl-L-tyramine (*N*-Boc-L-Tyr), were synthesized by photo-induced and thermal-induced polymerization, respectively, and were employed as the stationary phase in liquid chromatography. A stoichiometric displacement model for retention (SDM-R) was successfully constructed and applied to evaluate the chiral separation of the MIPs. The simulation results showed that the values of $\ln k'$ in the proposed SDM-R could be employed to characterize the efficiency of the MIP's total separation, and the value of n could be used to denote the space effect of the enantiomers interacting with the MIPs when the interaction between the solutes and MIPs was a hydrogen-bonding interaction. Further studies showed that the suitability of the MIP cavity structure mainly determined the chiral-recognition ability of the imprinting system, when a strong hydrogen-bond competitive solvent was added into the mobile phase.

Keywords: Chiral recognition; Molecular imprinting; Stoichiometric displacement model for retention (SDM-R)

1. Introduction

Molecular imprinting [1–5], which has received much attention in recent years, is a new and potential separation technique for preparing specialized recognition polymers. Although molecularly imprinted polymers (MIPs) have been used successfully in applications such as chromatography separation, solid extraction and mimicking enzymes and sensors, there are few reports on the chiral recognition mechanism [6–11]. Essentially, specialized interaction between imprinting molecules and MIPs is caused by both the complementary functional groups and the suited structures of the MIPs, but there are still very few studies on the relative intensity of these two factors.

This paper presents a study in which two kinds of MIPs were polymerized and chromatographic researches were performed in order to analyze the mechanism of the chiral recognition of MIPs. This study also established a new model for retention in molecular imprinting based on the stoichiometric displacement model for retention (SDM-R) in chromatography, and a simulation indicated that this method can determine the key factor affecting the chiral recognition of molecular imprinting.

2. Experimental

2.1. Materials and chemicals

N-Acetyl-DL-tryptophan (*N*-Ace-DL-Trp), *N*-carbobenzyloxy-DL-tryptophan (*N*-Cbz-DL-Trp), *N*-*tert*-butoxycarbonyl-D-phenylalanine (*N*-Boc-D-Phe), *N*-*tert*-butoxycarbonyl-L-phenyl-alanine (*N*-Boc-L-Phe), *N*-*tert*-butoxycarbonyl-

* Corresponding author. Tel.: +86 10 62788568; fax: +86 10 62770304.
** Co-corresponding author. Tel.: +86 10 62788568; fax: +86 10 62770304.
E-mail addresses: szy-dce@tsinghua.edu.cn (Z. Shen), yuhm@tsinghua.edu.cn (H. Yu).

0021-9673/$ – see front matter © 2004 Elsevier B.V. All rights reserved.
doi:10.1016/j.chroma.2004.08.161

L-tryptophan (*N*-Boc-L-Trp) and *N*-*tert*-butoxycarbonyl-L-tyramine (*N*-Boc-L-Tyr) were purchased from Sigma. *N*-*tert*-Butoxycarbonyl-D-tryptophan (*N*-Boc-D-Trp), *N*-*tert*-butoxycarbonyl-D-tyramine (*N*-Boc-D-Tyr) and ethylene glycol dimethacrylate (EDGMA) were purchased from Acros. Acrylamide, 2,2-azobis-(2-methylpropionitrile) (AIBN) and acetic acid were purchased from Beijing Chemical Reagent Plant. Methanol, alcohol, isopropyl alcohol, acetone and acetonitrile were all high performance liquid chromatography (HPLC) grade.

2.2. Equipment

The HPLC analysis was performed using an HPLC (Shimadzu) 10Avp. The column prepared for the molecular imprinting was packed with an air-driven fluid pump from Beijing Analytical Instrument Plant.

2.3. Preparation of molecularly imprinted polymers

2.3.1. Photo-induced polymerization

N-Boc-L-Trp (0.761 g, 2.5 mmol) and acrylamide (0.711 g, 10 mmol) were dissolved in acetonitrile (14.65 ml) and mixed at 4 °C for 12 h. Ethylene glycol dimethacrylate (9.44 ml, 50 mmol) and 100 mg of 2,2-azobis-(2-methylpropionitrile) were added to the acetonitrile which dissolved the *N*-Boc-L-Trp and acrylamide. The mixture was sonicated and deoxygenated with a stream of nitrogen, and then irradiated with UV light (365 nm) at 4 °C for 48 h. The process for the preparation of blank polymers was the same as that of the MIPs except that the imprinted molecules were not added in the polymerization process.

2.3.2. Thermal-induced polymerization

N-Boc-L-Tyr (0.703 g, 2.5 mmol) and acrylamide (0.711 g, 10 mmol) were dissolved in acetonitrile (14.65 ml) and mixed at 4 °C for 12 h. Ethylene glycol dimethacrylate (9.44 ml, 50 mmol) and 100 mg of 2,2-azobis-(2-methylpropionitrile) were added to the acetonitrile which dissolved the *N*-Boc-L-Tyr and acrylamide. The mixture was sonicated and deoxygenated with a stream of nitrogen, and then polymerized at 60 °C for 48 h. The process for the preparation of blank polymers was the same as that of the MIPs except that the imprinted molecules were not added during polymerization.

The bulk polymer was ground through a 30.8 μm sieve and sieved through a 38.5 μm sieve. The particles that passed through the 38.5 μm sieve but not the 30.8 μm sieve were collected and dried, then deposited in acetone many times. The small particles that did not deposit were discarded.

2.4. High performance liquid chromatography

The sieved and deposited MIPs of *N*-Boc-L-Trp and blank polymer particles were packed at 28 MPa into a stainless-steel HPLC column (250 mm × 4 mm, i.d.). Similarly, the sieved and deposited MIPs of *N*-Boc-L-Tyr and blank polymer particles were packed at 28 MPa into a stainless-steel HPLC column (250 mm × 4.6 mm, i.d.). Alcohol was used as the solvent. After being packed, the column was equilibrated with methanol–acetic acid (9:1, v/v) until a stable baseline was achieved.

The separation factor (α) was determined using the relationship $\alpha = k_L/k_D$, where k_L and k_D were the capacity factors of the L and D enantiomers, respectively. The capacity factors were determined according to $k_L = (t_L - t_0)/t_0$ and $k_D = (t_D - t_0)/t_0$, where t_L and t_D were the retention times of the L and D enantiomers, respectively, and t_0 was the retention time of the dead volume, which was determined by the injection of acetone. The resolution was denoted by *f*/*g* [12].

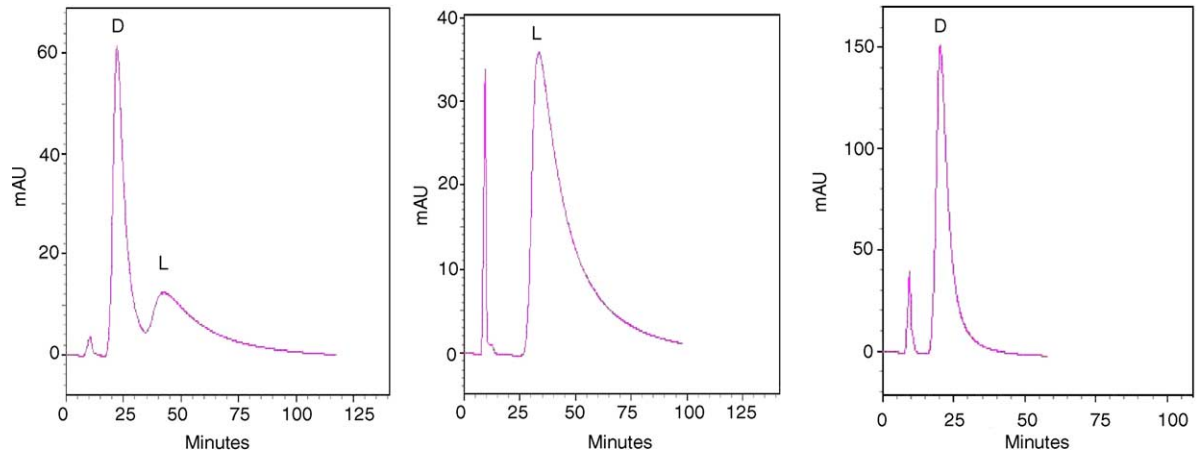

Fig. 1. MIPs evaluation by liquid chromatography. The eluent was acetonitrile, the flow rate was 0.3 ml/min, and the temperature was 27 °C. The racemic *N*-Boc-DL-Trp, *N*-Boc-L-Trp or *N*-boc-D-Trp were well resolved, and samples of 10 μl were injected into the chromatograph liquid.

Table 1
Results of chromatography for different substrates when applied to the corresponding L-selective polymers

	MIPs of *N*-Boc-L-Trp[a]			MIPs of *N*-Boc-L-Tyr[a]		
	k_D	k_L	α	k_D	k_L	α
N-Boc-DL-Trp	0.556	1.289	2.318	1.051	1.051	1
N-Boc-DL-Tyr				1.478	2.030	1.373
N-Cbz-DL-Trp	0.819	1.126	1.375			
N-Ace-DL-Trp	0.864	0.864	1			
N-Boc-DL-Phe	0.344	0.344	1	0.684	0.684	1

[a] For MIPs of *N*-Boc-L-Trp and *N*-Boc-L-Tyr, the eluent HAc was 4% and 0% in acetonitrile, respectively; the flow rates were 0.3 ml/min and 0.4 ml/min, respectively; the temperature was 27 °C; k_L was the capacity factor of L enantiomers; k_D was the capacity factor of D enantiomers; and α was the separation factor (k_L/k_D).

3. Results and discussion

3.1. Evaluation of MIPs by HPLC

In order to explore the chiral recognition mechanism of molecular imprinting, two kinds of MIPs, *N*-Boc-L-Trp and *N*-Boc-L-Tyr, were prepared. Correspondingly, the separation of racemic molecules, *N*-Boc-DL-Trp and *N*-Boc-DL-Tyr, in these two MIPs were analyzed by HPLC. As shown in Fig. 1, the retention time of the imprinted molecule, *N*-Boc-L-Trp, was longer than that of *N*-Boc-D-Trp, showing that imprinted molecules have stronger interaction with the MIPs. That is, the MIPs of *N*-Boc-L-Trp were able to specifically select the imprinted molecules other than their enantiomorph. In the chromatographic mode, such polymers resulted in near baseline separation of the enantiomers of the imprinted molecule. A separation factor of 2.63 and a resolution factor of 0.84 were obtained.

The results for *N*-Boc-L-Tyr were similar to those for *N*-Boc-L-Trp; that is, the MIPs of *N*-Boc-L-Tyr were also able to specifically select the imprinted molecules other than their enantiomorph.

The enantioselectivity of two MIPs of *N*-Boc-L-Trp and *N*-Boc-L-Tyr was further investigated using racemic mixtures of five different substrates: *N*-Boc-DL-Trp, *N*-Boc-DL-Tyr, *N*-Cbz-DL-Trp, *N*-Ace-DL-Trp and *N*-Boc-DL-Phe. The separation results are listed in Table 1, and Fig. 2 shows the sketch maps of the substrate-structure.

From the data shown in Table 1, it is obvious that the capacity factor of the imprinted molecule was the highest one in each of the MIPs, showing that the interaction between MIPs and imprinted molecules was the strongest, which resulted in the best chiral separation of both imprinted molecules, *N*-Boc-L-Trp and *N*-Boc-L-Tyr.

Further comparison showed that the separation factor of *N*-Cbz-DL-Trp in the *N*-Boc-L-Trp MIPs was also greater than 1.0, with the exception of the imprinted molecule, *N*-Boc-L-Trp. Molecular structure analyses indicated that *N*-Boc-Trp and *N*-Cbz-Trp not only both contained the same tryptophane group which was capable of matching with the functional group in MIPs, but *N*-Boc-Trp also contained a *tert*-butoxycarbonyl side chain group, and *N*-Cbz-Trp also contained a carbobenzyloxy side chain group. These side chain groups had similar hydrophobic intensity, and they both interacted with the cavities of MIPs. Therefore, weak separation of *N*-Cbz-DL-Trp also occurred in the MIPs of *N*-Boc-L-Trp.

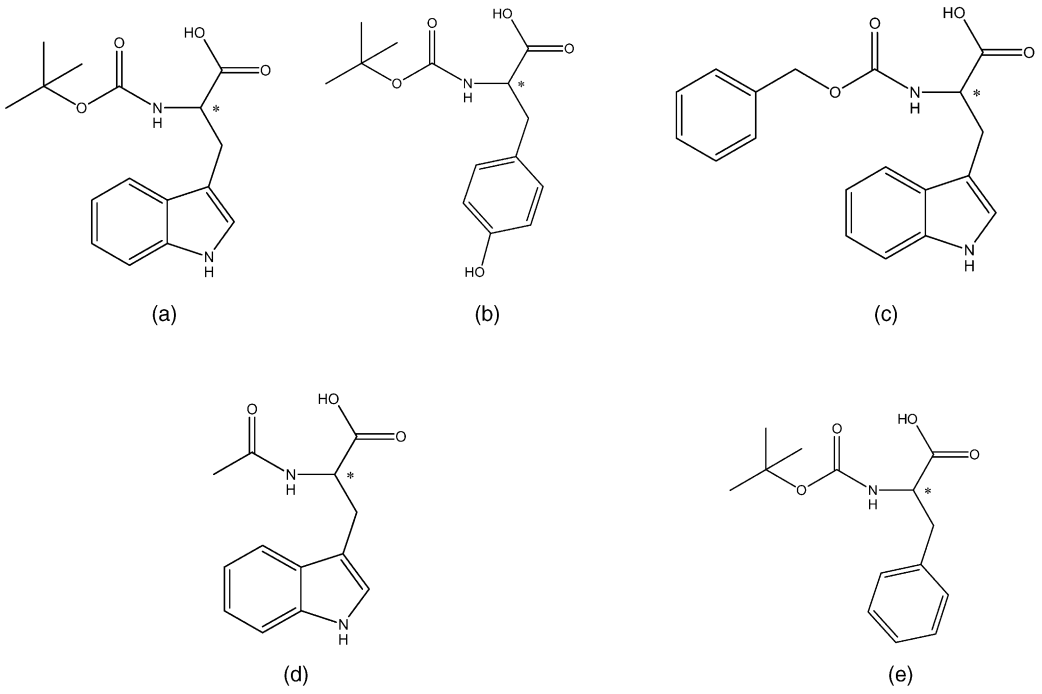

Fig. 2. Structure maps of five amino acid derivatives used in this study. (a) *N*-Boc-Trp; (b) *N*-Boc-Tyr; (c) *N*-Cbz-Trp; (d) *N*-Ace-Trp; and (e) *N*-Boc-Phe.

However, although both contained the same tryptophane, the *tert*-butoxycarbonyl group in *N*-Boc-Trp was much larger than acetyl in *N*-Ace-Trp, so the space structure of *N*-Ace-Trp did not match with the MIPs of *N*-Boc-L-Trp. For *N*-Boc-Phe, its phenyl group was much smaller than the indolyl group, and the phenyl group also had no nitrogen atom-forming hydrogen bond with the functional group of MIPs. Therefore, the MIPs of *N*-Boc-L-Trp could not separate *N*-Ace-DL-Trp and *N*-Boc-DL-Phe effectively.

For the MIPs of *N*-Boc-L-Tyr, *N*-Boc-Trp and *N*-Boc-Phe had no phenol group capable of matching with the functional group in MIPs. Thus, the MIPs of *N*-Boc-L-Tyr could not separate *N*-Boc-DL-Trp and *N*-Boc-DL-Phe effectively.

In short, the MIPs of *N*-Boc-L-Trp polymerized by photoinducement and the MIPs of *N*-Boc-L-Tyr polymerized by thermal-inducement both had the characteristics of selective specificity to the imprinted molecules, not only due to the complementary functional groups, but also due to the matched space structures; therefore they could be successfully used for the following studies of chiral recognition.

3.2. Interaction of the imprinted molecules, functional monomer and MIPs

Molecular simulations were carried out to determine the interaction between acrylamide and *N*-Boc-L-Trp. Their configurations were first optimized by ab initio prediction, then the interaction between them was investigated by a molecular dynamics simulation using the software HyperChem 7. The results showed that when there were one *N*-Boc-L-Trp and four acrylamide molecules in a system, the *N*-Boc-L-Trp could form 1:3 adducts with acrylamide and the main interaction between them was hydrogen bonding, showing that the interaction between the imprinted molecule *N*-Boc-L-Trp, and the functional monomer, acrylamide, is a hydrogen-bonding interaction.

Fig. 3 shows the polymerization processes of the MIPs of *N*-Boc-L-Trp and *N*-Boc-L-Tyr, indicating the hydrogen-binding interaction and the cavity structures.

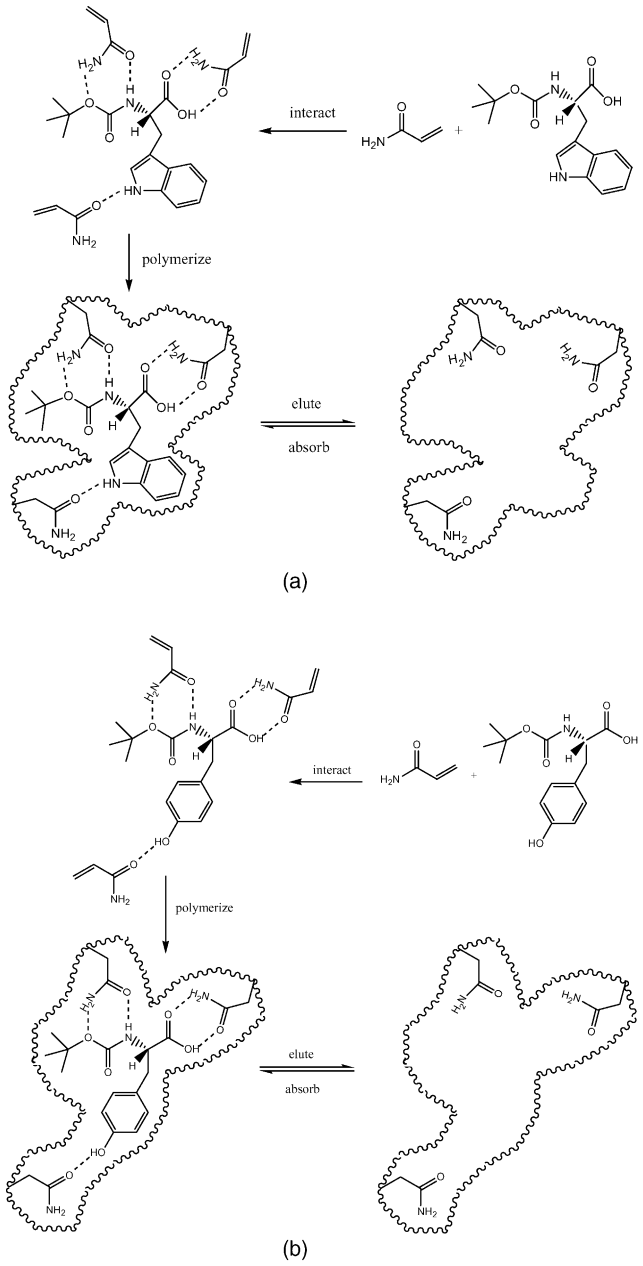

Fig. 3. Sketch map of the polymerization process of the MIPs of *N*-Boc-L-Trp and *N*-Boc-L-Tyr. (a) *N*-Boc-L-Trp and (b) *N*-Boc-L-Tyr.

3.3. Construction of an SDM-R model in molecular imprinting

Earlier studies by Mosbach and coworkers [9] and Lei and Tan [13], on the recognition mechanism of the molecular imprinting technique only considered the competitive adsorption between imprinted molecules and strong solvents on the MIPs, but the influence of weak solvents was ignored. The stoichiometric displacement model for retention [14] was a chromatography theory introduced in the 1980s and successfully used in reversed phase chromatography [15], normal chromatography [16], ion exchange chromatography [17], affinity chromatography [18], and some actual systems on the Chiralcel OJ Column [19,20]. Essentially, the molecular imprinting technique can be regarded as a new method of affinity chromatography, because the stationary phase, MIPs, can effectively adsorb the imprinted molecules through the interaction of the complementary functional groups of imprinted molecules and their matching MIP structure. Thus, SDM-R offers a new method to investigate the chiral recognition mechanism of molecular imprinting considering the influence of weak solvents.

The SDM-R theory makes the following assumptions:

(1) The solute retention mainly depends on a strong solvent, but it can also be affected by the competitive adsorption between weak and strong solvents in the stationary phase.
(2) The solvation among solvents can be ignored.

(3) In the stationary phase, one active site can only adsorb one solvent molecule, whereas one solute molecule should interact with several active sites.
(4) The solute molecules are ideal rigid molecules. That is, when the solute molecules are adsorbed on the surface of the stationary phase, their conformation does not change, so the solvation is the same as the non-adsorbed solute.

In the molecular imprinting system, one additional assumption should further be made:

(5) When solute molecules are adsorbed by the stationary phase, few solvent molecules are displaced from the solvated solute molecules.

Actually, when a solute molecule is adsorbed by the stationary phase, the number of solvent molecules that is displaced from the solute molecule is very small [21], and thus can be ignored.

From these assumptions, the equilibriums 1 and 2 below are obtained, where I denotes a strong solvent (displacing agent), L denotes the active site, LI is the complex between a strong solvent and the active site, W is a weak solvent, LW is the complex between a weak solvent and the active site, S is the solute, SI_m is the complex between the solute and a strong solvent, SL_nI_m is the complex among a strong solvent, the active site and the solute. Note: equilibrium 2 shows the process by which a weak solvent is displaced by a strong solvent.

$$SI_m + nLI \overset{K_1}{\rightleftharpoons} SL_nI_m + nI \quad (1)$$

$$I + LW \overset{K_2}{\rightleftharpoons} LI + W \quad (2)$$

The two equilibrium constants, K_1 and K_2, are:

$$K_1 = \frac{[SL_nI_m][I]^n}{[SI_m][LI]^n} \quad (3)$$

$$K_2 = \frac{[LI][W]}{[I][LW]} \quad (4)$$

Here, for the sake of convenience, the concentration is expressed as the volume percentage.

The distribution coefficient, K_d, can be expressed as:

$$K_d = \frac{[SL_nI_m]}{[SI_m]} \quad (5)$$

Based on Eqs. (4) and (5), Eq. (3) can be written as:

$$K_1 = \frac{K_d\{(K_2 - 1)[I] + 1\}^n}{K_2^n} \quad (6)$$

The capacity factor, k', is given by the following equation:

$$k' = K_d\varphi \quad (7)$$

where φ is the phase ratio of the column.

From (6) and (7), it can be deduced that:

$$\ln k' = \ln A - n\ln(1 + \beta[I]) \quad (8)$$

where $\ln A = \ln\varphi + \ln K_1 + n\ln K_2$ and $\beta = K_2 - 1$. Here β indicates the equilibrium constant of a weak solvent displaced by a strong solvent.

Eq. (8) is nonlinear, so it is difficult to accurately calculate each parameter by fitting experimental data [22].

From the studies of Geng Xindu and Bian Liujiao, β is less than 1 in the binary-component system [23]. Additonally, in the process of separation by molecular imprinting, the concentration of the strong hydrogen-bonding competitive solvent is usually very low in order to ensure chiral separation. For example, when the concentration of methanol was increased to only about 6% ([I] = 0.06, v/v) in the mobile phase, the MIPs lost their properties of chiral separation (Fig. 4).

Thus, in the study of the recognition mechanism, the concentration of the strong hydrogen-bonding competitive solvent should be less than 6%. When [I] ≤ 0.05 (v/v), the second right-hand logarithmic term of Eq. (8) can be expanded in progression in the following form:

$$\ln(1 + x) = x - \tfrac{1}{2}x^2 + \cdots, \quad 0 < X \leq 1 \quad (9)$$

Taking the first term of the expansion in equation (9), equation (8) can be quite definitely simplified as:

$$\ln k' = \ln A - n\beta[I] \quad (10)$$

where $\ln A = \ln\varphi + \ln K_1 + n\ln K_2$ and $\beta = K_2 - 1$.

Here $\ln A$ represents the total affinity potential between the solute and the stationary phase, which includes not only the space effect between the solute and the cavity structure of the MIPs, but also the interaction between solute, solvent and functional monomer.

Parameter n is the number of the strong solvent molecules released from the stationary phase when a solute molecule is adsorbed on the stationary phase. The value of n mainly depends on the kind of interaction and the osculated area between the solute and the stationary phase [15]. For the two

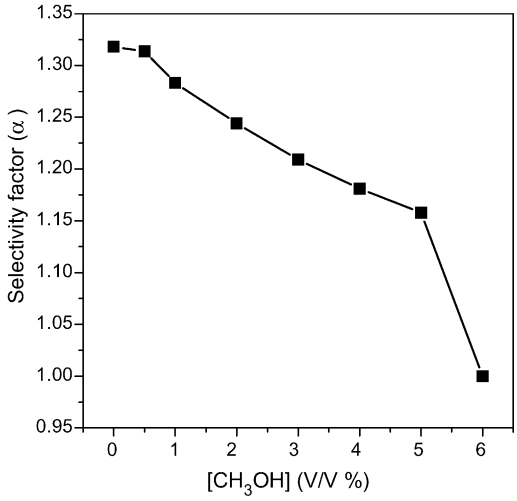

Fig. 4. Effect of methanol concentration on the selectivity factor. Experimental conditions were the same as Fig. 1.

Table 2
SDM-R results for photo-polymerized MIPs of *N*-Boc-L-Trp and blank polymers

Solute	ln *A*	*nβ*	*R*
MIPs of *N*-Boc-L-Trp			
N-Boc-D-Trp	0.214	13.702	−0.99943
N-Boc-L-Trp	1.174	17.571	−0.99771
N-Cbz-D-Trp	0.631	13.638	−0.99894
N-Cbz-L-Trp	1.041	16.591	−0.99945
N-Ace-DL-Trp	0.769	14.653	−0.99865
N-Boc-DL-Tyr	0.424	14.678	−0.99809
N-Boc-DL-Phe	−0.354	11.386	−0.99807
Blank polymers			
N-Boc-DL-Trp	−0.100	13.281	−0.99914
N-Cbz-DL-Trp	0.331	13.456	−0.99967
N-Ace-DL-Trp	0.380	12.972	−0.99959
N-Boc-DL-Tyr	0.132	14.281	−0.99843
N-Boc-DL-Phe	−0.567	12.470	−0.99727

MIPs of *N*-Boc-L-Trp and *N*-Boc-L-Tyr with acrylamide as the functional monomer, the main interaction is a hydrogen-bonding interaction, as discussed in previous section. Because the number of hydrogen bonds is approximately in direct ratio to the osculated area, the change of *n* mainly depends on the osculated area between the solute and the stationary phase. Therefore, the higher the value of *n* is, the larger the osculated area between the solute and the stationary phase is, and the more closely the MIP's cavity structure matches the solute.

Parameter β is a constant that is only related to the properties of the mobile and stationary phases in theory [23], because K_2 represents the equilibrium constant of the competitive adsorption between a strong solvent and a weak solvent.

3.4. Application of SDM-R in molecular imprinting with isopropyl alcohol as the strong solvent

Adding different concentrations of isopropyl alcohol into acetonitrile as a strong hydrogen-bonding competitive solvent, chromatography analyses were performed to simulate the SDM-R model. The figures of $\ln k'$ versus [I] fitted with Eq. (10) are plotted in Figs. 5 and 6. The numerical values of $\ln A$, $n\beta$ and the correlation coefficients, *R*, in different systems of MIPs, blank polymers and solutes were calculated, and are summarized in Tables 2 and 3.

These results revealed that:

Table 3
SDM-R results for thermal-polymerized MIPs of *N*-Boc-L-Tyr and blank polymers

Solute	ln *A*	*nβ*	*R*
MIPs of *N*-Boc-L-Tyr			
N-Boc-D-Tyr	0.409	15.632	−0.99908
N-Boc-L-Tyr	0.730	17.477	−0.99886
N-Boc-DL-Phe	−0.380	12.796	−0.99892
Blank polymers			
N-Boc-DL-Tyr	−0.285	14.837	−0.99669
N-Boc-DL-Phe	−0.988	11.442	−0.99528

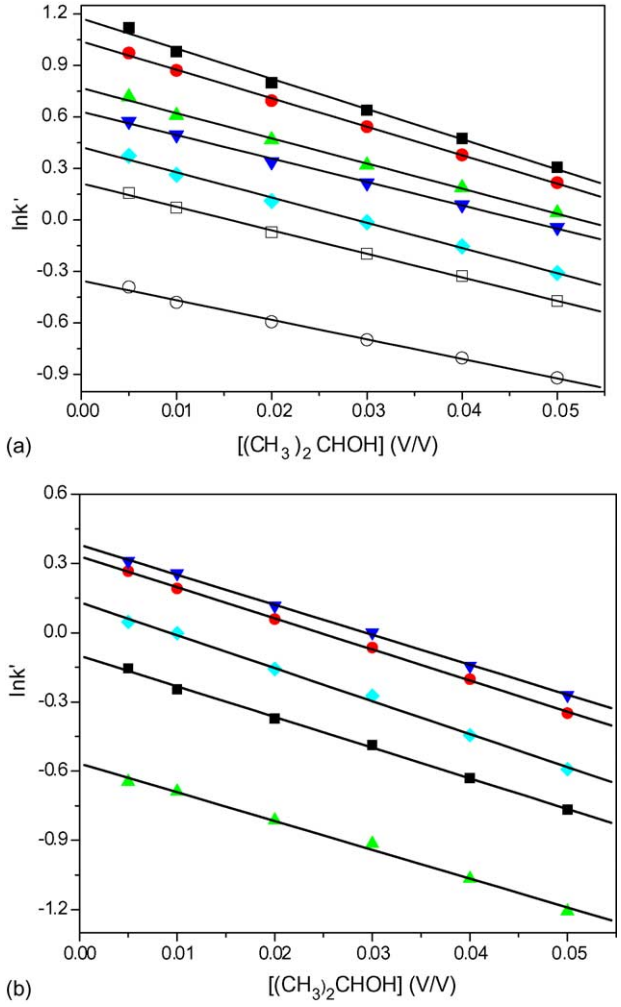

Fig. 5. Plot of $\ln k'$ vs. [I] fitted with Eq. (10) in the photo-induced polymerized MIP and blank polymer. The column temperature was 27 °C. The mobile phase was acetonitrile with 0.5%–5% (v/v) isopropyl alcohol, and the flow rate was 0.4 ml/min. (a) The stationary phase was the MIP of *N*-Boc-L-Trp, and the solutes were: (■) *N*-Boc-L-Trp, (▲) *N*-Cbz-L-Trp, (●) *N*-Ace-DL-Trp, (▼) *N*-Cbz-D-Trp, (◆) *N*-Boc-DL-Tyr, (□) *N*-Boc-D-Trp, and (○) *N*-Boc-DL-Phe. (b) The stationary phase was the blank polymer, and the solutes were: (■) *N*-Boc-DL-Trp, (▲) *N*-Cbz-DL-Trp, (●) *N*-Boc-DL-Phe, (▼) *N*-Ace-DL-Trp, and (◆) *N*-Boc-DL-Tyr.

(1) The absolute values of all of the correlation coefficients were higher than 0.99, which confirmed that the theory of SDM-R definitely could be successfully used in the technique of molecular imprinting with the MIPs of both photo-polymerized *N*-Boc-L-Trp and thermal-polymerized *N*-Boc-L-Tyr.
(2) For the MIPs of both *N*-Boc-L-Trp and *N*-Boc-L-Tyr, the $\ln A$ values of the imprinted molecules were the highest, and for all kinds of solutes, the $\ln A$ difference between the imprinted molecules of MIPs and of blank polymers were also the greatest, proving that $\ln A$ could be used to evaluate the separation characteristics of the MIPs.
(3) Of all of the solutes listed in Tables 2 and 3, $n\beta$ had the highest value for both imprinted molecules (*N*-Boc-

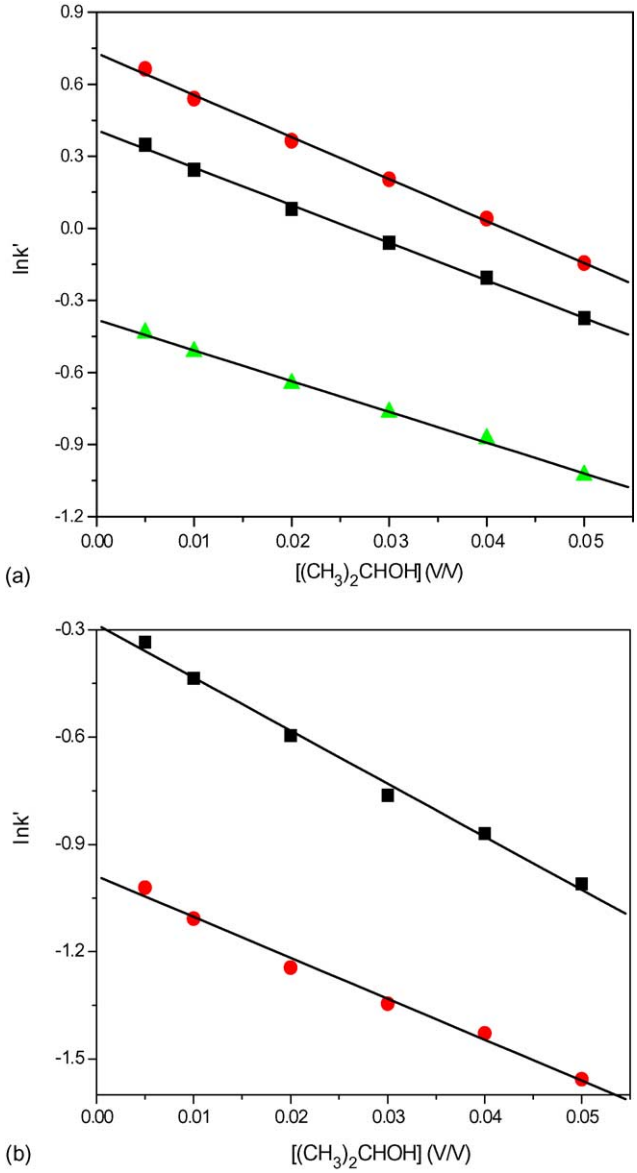

Fig. 6. Plot of $\ln k'$ vs. [I] fitted with Eq. (10) in the thermal-induced polymerized MIP and blank polymer. The column temperature was 27 °C. The mobile phase was acetonitrile with 0.5%–5% (v/v) isopropyl alcohol, and the flow rate was 0.4 ml/min. (a) The stationary phase was the MIP of *N*-Boc-L-Tyr, and the solutes were: (■) *N*-Boc-D-Tyr, (▲) *N*-Boc-L-Tyr, and (●) *N*-Boc-DL-Phe; (b) The stationary phase was the blank polymer, and the solutes were: (■) *N*-Boc-DL-Tyr and (●) *N*-Boc-DL-Phe.

L-Trp and *N*-Boc-L-Tyr). Because β was a constant in the above two systems using isopropyl alcohol as the strong solvent, the value of $n\beta$ was in direct proportion to n. Therefore, when different solute molecules were adsorbed on the stationary phase, the highest number of active sites were covered by the imprinted molecules, and the corresponding number of solvent molecules that were released from the stationary phase was also highest. That is, the structure of the imprinted molecules was more suited for the cavity structures of the MIPs. Because of the high similarity of the molecular structure to *N*-Boc-L-Trp, the value of n for *N*-Cbz-L-Trp was the second highest one in Table 2.

Table 4
Correlation of the ratio of n_{MIPs}/n_{blank} and the selectivity factor

MIPs	Solutes	n_{MIPs}/n_{blank}	α
N-Boc-L-Trp	*N*-Boc-DL-Trp	1.28	2.65
	N-Cbz-DL-Trp	1.22	1.51
N-Boc-L-Tyr	*N*-Boc-DL-Tyr	1.12	1.37

The retention of all kinds of solute molecules in blank polymers reflects the intrinsic adsorbing properties of polyacrylamide, whereas the retention of all kinds of solute molecules in MIPs reflects the adsorbing properties of MIPs. Therefore, the retention differences between MIPs and blank polymers can be considered to be caused by the influence of the imprinting process. As shown in Tables 2 and 3, the n values of two imprinted molecules and *N*-Cbz-L-Trp were higher in the MIPs than in the blank polymers, while for other kinds of solutes, the n values in MIPs and in blank polymers were almost the same. These results showed that it is the suited cavity structure of MIPs that increased the number of active sites adsorbing the imprinted molecules. Further studies showed that the higher the ratio of n in MIPs and in blank polymers (n_{MIPs}/n_{blank}), the higher the selectivity factor, α (as shown in Table 4). That is, the more closely the structure of the imprinted molecules matched with the cavity of the MIPs, the more effective the chiral separation of the racemic complex by the molecular imprinting technique was.

All these results indicated that parameter n could be used to evaluate the space effect of the enantiomers interacting with the MIPs when the interaction between the solutes and MIPs was a hydrogen-bonding interaction.

3.5. Application of SDM-R in molecular imprinting with different strong solvents

In general, the interaction between the imprinted molecules and MIPs in organic solvents is a hydrogen-bonding interaction [9]. Thus, the retention of the imprinted molecules changes when the strength of the hydrogen bond in the mobile phase is changed.

Different concentrations (0.5%–5%, v/v) of methanol, alcohol or isopropyl alcohol, which are three kinds of strong hydrogen-bond competitive solvents, were each added to acetonitrile to determine the effect of hydrogen bond strength on chiral recognition of molecular imprinting, and then the theory of SDM-R was used to simulate the experiments. The final fitting results for different mobile phase are listed in Table 5.

As shown in Table 5, the absolute values of all of the correlation coefficients were higher than 0.99, proving that the theory of SDM-R can be successfully used in the imprinting system with different hydrogen-bond strengths. Obviously, for different solutes in each mobile phase, the values of $\ln A$ of the imprinted molecules were the highest, indicating that

Table 5
SDM-R results for thermal-polymerized MIPs of *N*-Boc-L-Tyr when different strong solvents were added

	N-Boc-L-Tyr	*N*-Boc-D-Tyr	*N*-Boc-DL-Trp	*N*-Boc-DL-Phe
Strong solvent				
Methanol				
$\ln A$	0.662	0.383	0.126	−0.290
$n\beta$	27.516	24.740	22.193	21.184
R	−0.99919	−0.99929	−0.99936	−0.99943
Alcohol				
$\ln A$	0.603	0.346	0.106	−0.343
$n\beta$	20.626	18.794	17.205	15.909
R	−0.99896	−0.99932	−0.99714	−0.99953
Isopropyl alcohol				
$\ln A$	0.730	0.409	0.0579	−0.380
$n\beta$	17.477	15.632	13.030	12.796
R	−0.99886	−0.99908	−0.99915	−0.99892

the MIPs could accomplish chiral separation under different mobile phase conditions.

Additionally, because β is related to the competitive adsorption of strong solvents, β has the highest value for methanol; the value of $n\beta$ was higher in methanol than in alcohol or isopropyl alcohol, although the value of n decreased with the increasing strength of the hydrogen bond competition between the solvents and the MIPs. Further calculation, shown in Table 5, indicated that the ratio of $n\beta$ of the imprinted molecule to its enantiomorph was an approximate constant of 1.1 in the methanol, alcohol and isopropyl alcohol systems. In other words, for the MIPs of *N*-Boc-L-Tyr, when the strong solvents were changed in the mobile phase, the corresponding changing proportion of n of the imprinted molecules was equal to the molecule's enantiomorph. This result meant that when the interaction of the solutes and MIPs was decreased with the increasing ability of solvents to form hydrogen bonds in the mobile phase, the decrease of the imprinted molecule was in geometric proportion to the decrease in its enantiomer. That is, the molecular recognition of imprinted molecules and their enantiomorphs was mainly depended on how well the geometric cavity structures of MIPs suited with the structure of the imprinted molecules, when strong hydrogen-bond competitive solvents were added into the mobile phase.

Additional studies showed that the MIPs of *N*-Boc-L-Trp were very stable. The separation factor and resolution factor were independent of use-times before 350. After 350 times, these MIPs suddenly lost their chiral separation capability. Infrared spectrum analyses showed that the amide groups were still located in the MIPs. Thus, the reason for the loss of selectivity must be the changes of the structure of the MIPs. This result also indicated that the molecular recognition between imprinted molecules and MIPs mainly depended on how well the MIP's cavity structure was suited for the imprinted molecules. In order to further confirm this conclusion, we used 50 mmol/l phosphatic kalium as the mobile phase so that the cavity structure of the MIPs of *N*-Boc-L-Trp changed irreversibly. As expected, the MIPs lost their chiral separation capability, even though acetonitrile was used many times to balance the MIPs. Infrared spectrum analyses also showed that the loss of the chiral-separation ability was not caused by the loss of the amide groups, which further indicated that the chiral molecular recognition was mainly dependent on the suitability of the MIP's cavity structure in the molecular imprinting technique.

4. Conclusion

Two kinds of molecularly imprinted polymers, photopolymerized *N*-Boc-L-Trp and thermal-polymerized *N*-Boc-L-Tyr, were synthesized using acrylamide as the functional monomer. Both MIPs could efficiently separate the racemic amino acid derivatives. Results of molecular simulation showed that the interaction of the imprinted molecule and the functional monomer was mainly a hydrogen-bonding interaction, and a 1:3 adduct of *N*-Boc-L-Trp and acrylamide would be formed during the interaction. Based on several assumptions, a stoichiometric displacement model for retention was successfully introduced and constructed to further investigate the chiral recognition mechanism of the molecular imprinting technique. Further experiments confirmed that the SDM-R theory is doubtless applicable in the technique of molecular imprinting. The simulation results showed that the values of $\ln k'$ in SDM-R could be employed to characterize the total separation efficiency of MIPs, and the value of n could be used to denote the space effect of the solutes interacting with the MIPs. Further studies showed that the suitability of the MIPs' cavity structures mainly determined the chiral-recognition ability of the imprinting system. This means that the space effect is the major factor determining the chiral separation of MIPs, relative to the interaction of the enantiomers with MIPs. Therefore, a more rigid functional monomer should be selected in the polymerization of MIPs. Additionally, the application of SDM-R in the system of molecular imprinting will make it possible to quantitatively determine the contribution of different variables, and this will

consequently guide the selection of the functional monomer and the preparation of MIPs in theory, ultimately increasing the separation efficiency of the molecular imprinting system.

Acknowledgments

We thank Prof. Tan Tianwei and Dr. Dong Wenguo (Beijing University of Chemical Technology, China) for their kind assistance in column packing, and Prof. Liu Zheng (Tsinghua University, china) for his kind help in the molecular simulations.

References

[1] G. Wulff, Am. Chem. Soc. Symp. Ser. 308 (1986) 186.
[2] M. Kempe, K. Mosbach, J. Chromatogr. A 694 (1995) 3.
[3] G. Wulff, Angew Chem. Int. Ed. Eng. 34 (1995) 1812.
[4] K. Nilsson, K. Sakaguchi, J. Chromatogr. A 707 (1995) 199.
[5] G. Wullff, S. Schanhaff, J. Org. Chem. 56 (1991) 395.
[6] B. Sellergren, K.J. Shea, J. Chromatogr. A 654 (1993) 17.
[7] S. Vidyasankar, M. Ru, F.H. Arnold, J. Chromatogr. A 775 (1997) 51.
[8] J.F. Wang, L.M. Zhou, X.L. Liu, et al., Chem. J. Chin. Univ. 21 (2000) 930.
[9] B. Sellergren, M. Lepisto, K. Mosbach, J. Am. Chem. Soc. 110 (1988) 5853.
[10] Z.H. Meng, J.F. Wang, L.M. Zhou, et al., Anal. Sci. 15 (1999) 141.
[11] M.J. Whitcombe, L. Martin, E.N. Vulfson, Chromatography 47 (1998) 457.
[12] V.R. Meyer, Chromatography 24 (1987) 639.
[13] J.D. Lei, T.W. Tan, Biochem. Eng. J. 11 (2002) 175.
[14] X.D. Geng, L.J. Bian, Chin. Chem. Lett. 1 (1990) 135.
[15] G.H. Lei, H.Y. Zhu, X.D. Geng, J. Northwest Univ. (China) 27 (1997) 326.
[16] Z.H. Song, X.D. Geng, Acta Chim. Sinica (China) 48 (1990) 237.
[17] R.R. Drager, F.E. Regnier, J. Chromatogr. 359 (1986) 147.
[18] D.J. Anderson, R.R. Walters, J. Chromatogr. 331 (1985) 1.
[19] F. Yang, S.C. Wang, L.C. He, J. Xian Jiaotong Univ. (Med. Ed.) 25 (2004) 124.
[20] L. Gong, S.C. Wang, L.C. He, Chin. J. Pharm. Anal. 23 (2003) 399.
[21] R.F. Sun, H. Luo, H.Y. Sui, Z.Y. Shen, Chin. J. Proc. Eng. 3 (2003) 165.
[22] Y. Wang, J. Zhang, X.D. Geng, Chin. J. Chromatogr. 17 (1999) 326.
[23] X.D. Geng, L.J. Bian, Sci. China (Ser. B) 9 (1991) 915.